Optics Communications 403 (2017) 92–96

Contents lists available at ScienceDirect

Optics Communications

journal homepage: www.elsevier.com/locate/optcom

# Improved resolution and sensitivity of angular rotation measurement using entangled coherent states

Zijing Zhang [a,*], Tianyuan Qiao [a], Jie Song [a,*], Longzhu Cen [a], Jiandong Zhang [a], Shuo Li [a], Linyu Yan [a], Feng Wang [b], Yuan Zhao [a]

[a] Department of Physics, Harbin Institute of Technology, Harbin 150001, China
[b] Tianjin Jinhang Institute of Technology Physical, Tianjin 300192, China

ARTICLE INFO

*Keywords:*
Quantum interference measurement
Resolution
Parity detection

ABSTRACT

The performance of entangled coherent states for super-resolving angular-rotation measurement is investigated in this paper. Entangled coherent states with nonzero orbital angular momentum are first used as the input state, and parity detection method is adopted for signal processing. Analytical expressions of the output signal are derived. Numerical results show that the resolution and sensitivity of angular-rotation measurement using entangled coherent states are further enhanced relatively to those using classical coherent states. Moreover, this paper gives a detailed discussion about the impact of photon loss on the resolution and sensitivity of angular-rotation measurement.



## 1. Introduction

Precision measurements are of importance throughout all the fields of science and technology. There is a current significant interest in precision angular-rotation measurement which uses photon orbital angular momentum (OAM) to realize the improvement of the sensitivity and resolution [1–4]. Photon orbital angular momentum acts as a 'photonic gear', converting a mechanical rotation of an angular $\theta$ into an amplified rotation of the optical polarization by $l\theta$ with the quanta number $l$ of OAM [1]. Then, the sensitivity limit of angular-rotation measurement based on OAM is given, $1/\sqrt{Nl}$ for $N$ untangled photons and $1/Nl$ for $N$entangled photons [2]. Recently, Jha et al. employ a $4 \times 4$ matrix formulation to study the propagation of entangled OAM modes, and obtain explicit expressions for the resolution and sensitivity of angular-rotation measurement based on entangled OAM [3]. Through transferring polarization entanglement to OAM with an interferometric scheme, the experiment results demonstrate that the entanglement of high OAM can improve the sensitivity of angular-rotation measurement [4].

However many kinds of non-classical entanglement states are very sensitive to photon loss. They degrade rapidly under photon loss, which makes it difficult to achieve ultra-sensitivity and super-resolution in a lossy environment [5–9]. Recently, the entangled coherent states (ECS), a specific coherent superposition like NOON state, are proposed. Coherent states are known as the most "classical-like" quantum states, therefore ECS are very robust and useful [10–12]. This paper is different from our previous works [13,14], Entangled Coherent States (ECS) instead of Classical Coherent State (CCS) as the signal source is discussed in the precision angular rotation measurement. First, utilizing the general expression of the conditional probabilities, analytical expressions for the output signal and the sensitivity of angular-rotation measurement are derived with parity detection method. Then, the resolution and sensitivity of angular-rotation measurement using ECS are compared with those of classical coherent states through the numerical calculation. Finally, the effect of photon loss on the resolution and sensitivity is discussed.

## 2. Theoretical analysis

The scheme of angular-rotation measurement using ECS is depicted in Fig. 1. Three steps are included: first, the input state $\hat{\rho}_{in}$ of ECS is prepared; second, the input state $\hat{\rho}_{in}$ evolves to the output state $\hat{\rho}_{out}$ with the angular-rotation $\theta$-dependent dynamical process; finally, a measurement is made on the output state $\hat{\rho}_{out}$.

The first step (ready the ECS input state $\hat{\rho}_{in}$): A coherent superposition state (CSS) $|CSS\rangle = K\left(\left|\alpha/\sqrt{2}\right\rangle + \left|-\alpha/\sqrt{2}\right\rangle\right)$, with the normalized coefficient $K = \left[2\left(1+e^{-|\alpha|^2}\right)\right]^{-1/2}$ and the amplitude $\alpha = \sqrt{N}$, is injected into one input port '$a$'. Then, CSS carries the OAM of $+l$ after the modulation of q-plate 1 (Q1) [15,16], expressed as $|CSS\rangle_{a,+l} =$

* Corresponding authors. Fax: +86-451-86414129.
*E-mail addresses:* zhangzijing@hit.edu.cn (Z. Zhang), jiesong2002@gmail.com (J. Song).

http://dx.doi.org/10.1016/j.optcom.2017.07.024
Received 14 March 2017; Received in revised form 6 July 2017; Accepted 7 July 2017
0030-4018/

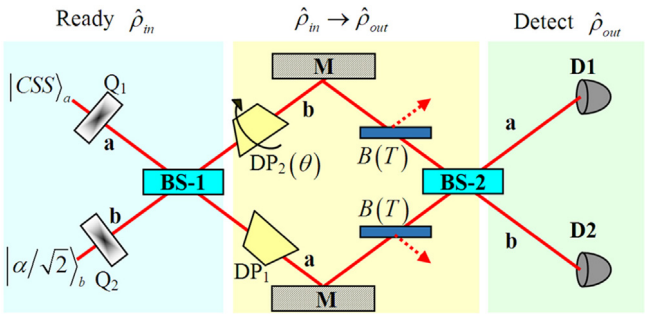


**Fig. 1.** Scheme of angular rotation measurement using ECS. CSS: coherent superposition states; Q: q-plate; BS: beam splitter; DP: Dove prism; M: Mirror; D: Detector.

$K\left(|\alpha/\sqrt{2}\rangle_{a,+l} + |-\alpha/\sqrt{2}\rangle_{a,+l}\right)$. In the other input port '$b$', a classical coherent state $|\alpha/\sqrt{2}\rangle$ goes through q-plate 2 (Q2) and carries the OAM of $-l$, expressed as $|\alpha/\sqrt{2}\rangle_{b,-l}$. The input signals of two paths are fed into the first 50:50 beam splitter BS-1 and become the ECS $|ECS\rangle = K\left(|\alpha\rangle_{a,+l}|0\rangle_{b,-l} + |0\rangle_{a,+l}|\alpha\rangle_{b,-l}\right)$ [17] ($|ECS\rangle$ is also experimentally available [18–21]). The density operator of the ECS input state is given by $\hat{\rho}_{in} = |ECS\rangle\langle ECS|$.

The second step (the $\theta$-dependent dynamical process $\hat{\rho}_{in} \to \hat{\rho}_{out}$): The clockwise light path is the detection light path, labeled as '$b$' and Dove prism DP2 is used to introduce an angular rotation of $\theta$, expressed by $\hat{U}(\theta) = \exp\left(i2l\theta\hat{N}_b\right)$ with the number operator $\hat{N}_b = \hat{b}^\dagger\hat{b}$. While the counter-clockwise light path is the reference light path, labeled as '$a$', and the angular of Dove prism DP1 is constant $\theta = 0$. The role of DP1 ensures that the helical wave front of each beam has the same sense, and thus interference between the beams is uniform across the whole aperture of detector. The fictitious beam splitter $\hat{B}(T)$ is used to model photon loss, with transmission coefficients $T$ [22]. The second 50:50 beam splitter is denoted by a unitary operator $\hat{B}_{1/2}$ [10]. The evolution process $\hat{\rho}_{in} \to \hat{\rho}_{out}$ can be described by an unitary transformation $\hat{M} = \hat{B}_{1/2}\hat{B}_b(T)\hat{B}_a(T)\hat{U}(\theta)$, and then the output state $\hat{\rho}_{out}$ is obtained

$$\begin{aligned}\hat{\rho}_{out} &= Tr\left(\hat{M}\hat{\rho}_{in}\hat{M}^\dagger\right)\\ &= |K|^2\begin{Bmatrix}|\beta\rangle_{a,+l}|i\beta\rangle_{b,-l}\,{}_{b,-l}\langle i\beta|_{a,+l}\langle\beta|\\ +\left|i\beta e^{i2l\theta}\right\rangle_{a,+l}\left|\beta e^{i2l\theta}\right\rangle_{b,-l}\,{}_{b,-l}\left\langle\beta e^{i2l\theta}\right|_{a,+l}\left\langle i\beta e^{i2l\theta}\right|\\ +e^{-R|\alpha|^2}\left(|\beta\rangle_{a,+l}|i\beta\rangle_{b,-l}\,{}_{b,-l}\left\langle\beta e^{i2l\theta}\right|_{a,+l}\left\langle i\beta e^{i2l\theta}\right| + H.c.\right)\end{Bmatrix}\end{aligned} \quad (1)$$

where, $\beta = \alpha\sqrt{T/2}$, and $R = 1 - T$. It is easy to see that the amplitudes in the output ports are reduced from $\alpha/\sqrt{2}$ to $\alpha\sqrt{T/2}$ with photon loss. More importantly, photon loss suppresses the off-diagonal coherence by a factor of $e^{-R|\alpha|^2}$, which is an important reason of the performance degeneration.

The third step (detect the output state $\hat{\rho}_{out}$): the output state $\hat{\rho}_{out}$ is projected into the two-mode Fock states $|n,m\rangle = |n\rangle_a|m\rangle_b$. The probability for detecting $n$ photons at the output port $a$ and $m$ photons at the output port $b$, $P(n,m) = \langle n,m|\hat{\rho}_{out}|n,m\rangle$, is given by

$$\begin{aligned}P(n,m) &= |K|^2\left\{2e^{-2|\beta|^2}|\beta|^{2(n+m)}/(n!m!)\right.\\ &\left.+e^{-|\alpha|^2}\left[\left(-i|\beta|^2e^{-i2l\theta}\right)^n\left(i|\beta|^2e^{-i2l\theta}\right)^m/(n!m!) + H.c.\right]\right\}.\end{aligned} \quad (2)$$

Considering either output port $a$ (or $b$), here we take the output port $a$ as an example. Summing over $m$, we obtain

$$\begin{aligned}P(n) &= |K|^2\left\{2e^{-|\beta|^2}|\beta|^{2n}/n!\right.\\ &\left.+e^{-|\alpha|^2}\left[e^{i|\beta|^2e^{-i2l\theta}}\left(-i|\beta|^2e^{-i2l\theta}\right)^n/n! + H.c.\right]\right\}.\end{aligned} \quad (3)$$

Parity detection was originally proposed in the context of trapped ions by Bollinger et al. in 1996 [23], described by a parity operator $\hat{\Pi}_a = (-1)^{\hat{n}_a} = e^{i\pi\hat{a}^\dagger\hat{a}}$. The experiment and theory of the parity detection method have been widely discussed [24,25]. Parity detection divides photon number $n$ into binary outcomes $\pm$ according to the even or odd of photon number $n$. If $n$ is even number, $\prod = +$; otherwise $\prod = -$. The conditional probability $P(\pm)$ can be obtained through a sum of $P(n)$ over the odd or even of the photon number $n$

$$\begin{aligned}P(\pm) &= \sum_n^{even/odd n} P(n)\\ &= \frac{1}{2} \pm |K|^2\left[e^{-T|\alpha|^2} + e^{-|\alpha|^2[1-T\sin(2l\theta)]}\cos\left(T|\alpha|^2\cos(2l\theta)\right)\right].\end{aligned} \quad (4)$$

One can note that $P(+) + P(-) = 1$, and

$$\begin{aligned}\left\langle\hat{\prod}\right\rangle &= P(+) - P(-)\\ &= 2|K|^2\left[e^{-T|\alpha|^2} + e^{-|\alpha|^2[1-T\sin(2l\theta)]}\cos\left(T|\alpha|^2\cos(2l\theta)\right)\right].\end{aligned} \quad (5)$$

This is the analytical expression of the output signal, which agrees with the results of [26]. There are two terms in Eq. (5): the first one is a constant term which only affects the basal amplitude of the output signal; the second one is the interferometric term which determines the sensitivity and resolution of angular rotation measurement. Where, the exponential part $e^{-|\alpha|^2[1-T\sin(2l\theta)]}$ quantifies the coherence of ECS.

Next, the sensitivity is estimated via the quantum estimation theory $\delta\theta_{\prod} = \Delta\hat{\prod}/\left|\mathrm{d}\left\langle\hat{\prod}\right\rangle/\mathrm{d}\theta\right|$ [27,28]. Here, $\Delta\hat{\prod} = \sqrt{\left\langle\hat{\prod}^2\right\rangle - \left\langle\hat{\prod}\right\rangle^2} = \sqrt{1 - \left\langle\hat{\prod}\right\rangle^2}$ with $\hat{\prod}^2 = 1$. $\delta\theta_{\prod}$ is given by Eq. (6) (see Box I)).

## 3. The resolution and sensitivity of ECS

Figs. 2(a)–(c) depict normalized output signals of ECS (the red solid lines) and CCS (the blue dashed lines) under different values of average photon number $N$ and OAM quanta number $l$. With the same signal processing method of parity detection, the signal peaks of ECS are narrower than the ones of CCS, which means better resolution. Comparing Figs. 2(a) and (b), with the increase of OAM quanta number $l$, the signal peaks of both ECS and CCS become narrower. Comparing Figs. 2(a) and (c), with the increase of average photon number $N$, ECS will appear multiple narrow peaks and result in $\sqrt{N}$ times narrower than CCS due to the double cosine modulation in the second term of Eq. (5). In Fig. 2(d), it can be seen that FWHMs (full width at half maximum) of ECS and CCS decrease with the increase of average photon number $N$ and OAM quanta number $l$, and FWHM of ECS is always less than that of CCS. This shows that ECS can further improve the resolution of angular rotation measurement compared with CCS due to the entanglement properties.

Fig. 3 discusses the sensitivity of angular rotation measurement using ECS and CCS. In Fig. 3(a), the blue dashed line represents the sensitivity of CCS, while the red solid line represents the sensitivity of ECS. The best sensitivity $\delta\theta_{\min}$ means the minimum value of sensitivity curves which can be obtained by choosing the appropriate angle $\theta$. The best sensitivity of ECS will appear at $\theta = \pi/4l$, and the reason is that the exponential part $e^{-|\alpha|^2[1-T\sin(2l\theta)]}$ is maximum when $\theta = \pi/4l$, which means the best coherence. Here, the sensitivity curves of ECS are shifted $\theta = \pi/4l$ along the $\theta$ axis (all of the following plots in this paper take the same manipulation), in order to be convenient for comparison with CCS. It is easy to see that the best sensitivity of ECS is superior to that of CCS. For the interference measurements, no matter using either ECS or CCS, there are the corresponding ranges in which the best sensitivity can be obtained, not in the whole angle ranges. ECS has multiple narrow peaks, and in the corresponding ranges of multiple narrow peaks, the sensitivity of ECS is better than that of CCS. The best sensitivity of ECS is in the middle main peak and the range of middle main peak is also biggest, and therefore the range of middle main peak will be used in measurement. More details about the best sensitivity of ECS and CCS are shown in Fig. 3(b). The best sensitivity of ECS and CCS can be improved by increasing average photon number $N$ and the OAM quanta number $l$, and the best sensitivity of ECS is always better than that of CCS.